Journal of Theoretical and Computational Chemistry
Vol. 6, No. 3 (2007) 585–594

THE INVESTIGATION ON ELECTRONIC STRUCTURE AND SECOND-ORDER NONLINEAR OPTICAL PROPERTIES OF II–VI SEMICONDUCTOR CLUSTERS BY TIME-DEPENDENT DENSITY FUNCTIONAL THEORY

YONGQING QIU, XIAOHONG WANG and YICHUN LIU*

Key Laboratory of Excited State Physics
Changchun Institute of Optics Fine Mechanics and Physics
Chinese Academy of Sciences, Changchun 130021
People's Republic of China

Center for Advanced Opto-Electronic Functional Materials Research
Northeast Normal University, Changchun 130024
People's Republic of China
**ycliu@nenu.edu.cn*

GUOCHUN YANG and HUI CHEN

Institute of Functional Material Chemistry
Faculty of Chemistry, Northeast Normal University
Changchun 130024, People's Republic of China

Received 15 November 2006
Accepted 29 April 2007

Time-dependent density functional theory (TD-DFT) formalism is employed to calculate the electronic spectra of A_3B_3 II–VI semiconductor clusters based on the geometrical structures optimized at DFT-B3LYP level. Moreover, their second-order nonlinear optical (NLO) properties are performed by TD-B3LYP combined with sum-over-states (SOS) formula. The calculation results indicate that it is necessary to consider the effective core potential and electron correlation effects when the basis sets are chosen for the heavy atoms. In addition, the results show that the transition energies and HOMO–LUMO gaps of the A_3B_3 II–VI semiconductor clusters decrease, while the second-order nonlinear optical responses increase with the increasing of VI-group ionic radius. As a result, the SOS formula is valuable to calculate the β_μ in the summation of 120 states. Meanwhile, charge transfers from the π bonding to π anti-bonding orbitals between II and VI group atoms significantly contribute to the second-order NLO properties.

Keywords: II–VI semiconductor clusters; electronic structure; second-order NLO; TD-DFT.

*Corresponding author.

1. Introduction

II–VI semiconductor materials, such as ZnO, with photonic bandgaps and excitonic coupling energies, provide convenience to study the properties of exciton and short wavelength photoelectricity crystal. The semiconductor materials have been applied in many fields like ultraviolet laser emission crystal, piezocrystal, lightwave circuit, and high quantum dots luminescence crystal.[1–7] Recently, there has been a growing interest in the study of II–VI semiconductor cluster materials with nanostructure,[2–4] because the properties of clusters are remarkably different from those of the bulk materials.[8] For example, the cluster-assembled materials have novel mechanical, electrical, and optical properties.[9–11] Therefore, differentiating the nature of those differences between the cluster and the bulk is an important scientific problem to be solved. Due to the difference of the energy band structure and the phonon distribution between the clusters and crystalline bulk, clusters of a semiconductor may be optically active, but the bulk material is not. Meanwhile, clusters have localized states. The transition from an upper energy state to a lower one may contain one or more located intermediate states.

Experimental information about cluster structure may be obtained mainly based on the indirect measurements, such as optical absorption or luminescence spectrum. Accordingly, theoretical calculations for linear and nonlinear optical properties are particularly important and interesting. Korambath and Karna[12] employed the time-dependent Hartree–Fock (TD-HF) method to calculate the hyperpolarizabilities of GaX (X = N, P, and As) cluster. Vasiliev and co-workers[13] used a time-dependent density functional theory (TD-DFT) formalism within the local density approximation to calculate the absorption spectra of Ga_nAs_m clusters. In addition, Lan and Cheng *et al.*[14] employed TD-HF formalism combined with sum-over-states (SOS) method to calculate the linear and nonlinear optical properties of III–V semiconductor clusters as Ga_3As_3 and In_3P_3. However, there are a few reports about the theoretical research of II–VI semiconductor clusters. In this paper, the electronic structures and nonlinear optical properties of A_3B_3 II–VI semiconductor clusters were carried out by using TD-B3LYP method with SOS formula.

2. Computational Procedures and Models

For obtaining reliable ground state geometries of all clusters, the theoretical methods, relativistic effects of heavy atoms and basis set effects of all atoms should be considered. Considering the relativistic effects of heavy atoms, the ECP-121G basis set containing effective core potential (ECP) representations of electrons near the nuclei was applied of heavy atoms. DFT-B3LYP with different basis sets was employed to optimize the geometries of all clusters (see Table 1). In order to determine the optical properties of the clusters, it is necessary to know the eigenvalues and transition matrix elements of the ground and excited states for the clusters, which are related to the corresponding electronic wavefunctions. Accordingly, time-dependent density functional theory (TD-DFT) method was adopted to obtain the

Table 1. B3LYP optimized bond length (in Angstrom) and bond angles (in degree) for Zn_3O_3 and Zn_3S_3 as a function of basis set.

	Clusters	Crystal Parameters[a]	3-21G*	6-31G*	CEPI[b]	CEPII[c]	CEP-121G
Zn_3O_3	Zn–O	2.005	1.782	1.777	1.857	1.859	1.873
	Zn-O-Zn (O–Zn–O)	109.471	104.657	105.361	106.059	105.956	106.051
Zn_3S_3	Zn–S	2.342	2.121	2.206	2.227	2.234	2.262
	Zn-S-Zn (D–Zn–S)	109.471	109.096	109.886	110.071	110.135	110.367

[a]Data taken from crystal data.
[b]CEPI = CEP-121G for Zn and 3-21G* for O and S.
[c]CEPII = CEP-121G for Zn and 6-31G* for O and S.

molecular electronic spectra of all clusters based on the optimized reliable geometrical structures (see Sec. 3). The monoexcited configuration interaction approximation was employed to describe the excited states. Within TD-B3LYP calculations, the core electrons were frozen and inner-shells were excluded from the correlation calculations. The wavefunctions and energy eigenvalues of the excited states were determined by solving the time dependence Hartree–Fock equation. Moreover, the ECP basis sets involving the triplet split-valence of effective core potential were used[16,17] to calculate the spectra of II–VI semiconductor clusters. Finally, the second-order NLO properties were calculated by TD-B3LYP method combined with SOS formalism for those clusters.

The static and frequency-dependent second-order nonlinear optical polarizabilities were obtained by using the SOS method. The expression of second-order polarizability component of β_{ijk} was derived from the perturbation theory through Eq. (1), and assuming electric dipole coupling between the radiation field and the molecule.[18]

$$\beta_{ijk} = \frac{1}{4\hbar^2} P(i,j,k;-\omega_\sigma,\omega_1,\omega_2) \sum_{m\neq g} \sum_{n\neq g} \left[\frac{\langle g|\mu_i|m\rangle\langle m|\mu_j^*|n\rangle\langle n|\mu_k|g\rangle}{(\omega_{mg}-\omega_\sigma-i\Gamma_{mg})(\omega_{ng}-\omega_1-i\Gamma_{ng})} \right]. \tag{1}$$

Here, $\langle g|\mu_i|m\rangle$ is an electronic transition moment along the i-axis of the Cartesian system, between the ground state $\langle g|$ and the excited state $|m\rangle$; $\langle m|\mu_j^*|n\rangle$ denotes the dipole difference operator which equals to $[\langle m|\mu_j|n\rangle - \langle g|\mu_j|g\rangle\delta_{mn}]$; ω_{mg} is the transition energy; ω_1 and ω_2 are the frequencies of the perturbation radiation fields, $\omega_\sigma = \omega_1 + \omega_2$ being the polarization response frequency; $P(i,j,k;-\omega_\sigma,\omega_1,\omega_2)$ indicates that all permutations of ω_1, ω_2, and ω_σ along with associated indices i,j,k; Γ_{mg} is the damping factor. The transition energy, transition moments, and dipole moments can be obtained from the calculated results on the basis of the TD-B3LYP model. First, 100 excited states were calculated using the TD-B3LYP model for all compounds. Those physical values were then taken as an input of the SOS formula to calculate the second-order polarizabilities.

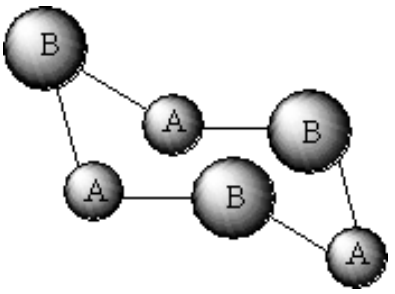

Fig. 1. The geometrical structures of the clusters used in the calculations (A = Zn, B = O, S, Se, Te; A = Cd, B = S, Se, Te; A = Hg, B = S, Se, Te).

It is well known that the zinc blende structures of II–VI semiconductor compounds have the cubic symmetry. The cluster structures studied in this paper are obtained by intercepting unit along (111) direction from the zinc blende structures. Thus, these clusters belong to C_{3v} symmetry point group, which are similar to the stable chair conformation of cyclohexane as shown in Fig. 1.

3. Results and Discussion

To identify the rationality of the chosen basis sets, Table 1 lists the B3LYP optimized geometrical parameters of Zn_3O_3 and Zn_3S_3 as a function of basis sets, those from the crystal structure being also given for comparison. The results show that the calculated distances are shortened by about 0.22 Å (in comparison to the crystal parameters) when the 3-21G* and 6-31G* basis sets are used for Zn and O, respectively. The same results reveal a significant lengthening (by ∼0.14 Å) on the optimized bond length with the use of both 3-21G* and 6-31G* for the O atom, the Zn one being treated with CEP-121G basis set. Note that the same observations in the trend of the Zn–O bond length were also made for Zn–S. In comparison with experimental data, the most reliable optimized structures for Zn_3O_3 and Zn_3S_3 are obtained with B3LYP/CEP-121G method, implying that the effective core potential and electronic correlation effects containing d or f electrons is necessary for Zn, while O and S are less basis set sensitive. The same trend is observed in the other clusters under investigation in this work. Consequently, we based below studies on the geometrical structures computed with CEP-121G basis set on heavy atoms and 6-31G* on the O and S atoms.

According to the type of cation, the 10 clusters can be classified into three categories: (a) Zn_3O_3–Zn_3Te_3, (b) Cd_3S_3–Cd_3Te_3, and (c) Hg_3S_3–Hg_3Te_3. Figure 2 shows their electronic spectra computed with TD-B3LYP/CEP-121G method. Based on the computational results, it can be found that the spectra of these clusters exhibit long absorption tails, which extend deeply into the region with low transition energies. Due to the rule of electronic transition and to the request of the orbital symmetry, the lowest electronic transitions energies are electronic dipole forbidden.

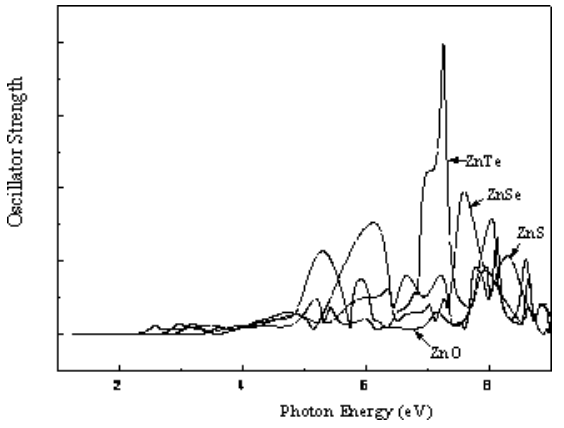

(a)

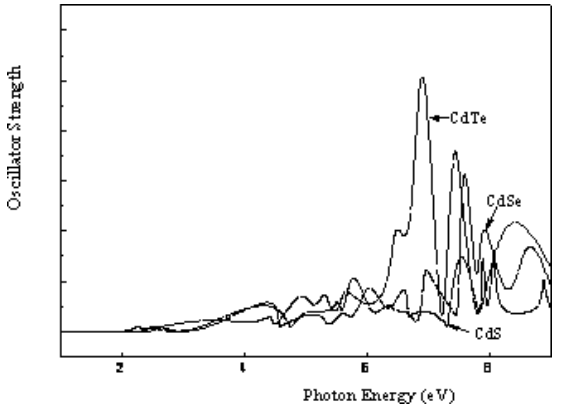

(b)

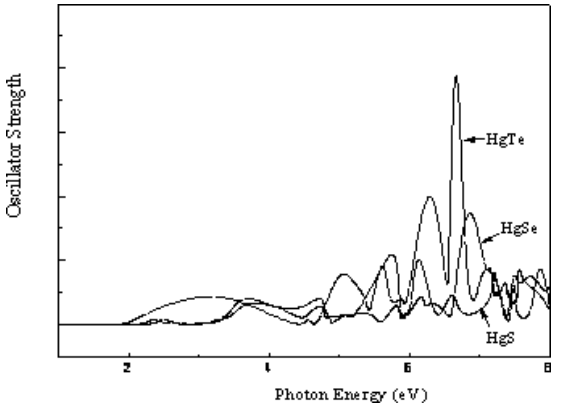

(c)

Fig. 2. The calculated absorption spectra of A_3B_3 clusters based on TD-B3LYP at CEP-121G level.

Table 2. The allowed transition energies (ΔE_{AT}), HOMO–LUMO gaps energies (ΔE_G) at ground state cluster, and the energy deference between the ground state and the first excitation state of cluster (ΔE_{FT}) for the 10 clusters.*

Clusters	Energy (eV)		
	ΔE_{AT}	ΔE_G	ΔE_{FT}
Zn_3O_3	3.6612 (0.0273)	2.744	1.6028 (0.000)
Zn_3S_3	3.1650 (0.0340)	1.904	1.0701 (0.000)
Zn_3Se_3	2.9626 (0.0346)	1.556	0.7559 (0.000)
Zn_3Te_3	2.6091 (0.0355)	1.138	0.3893 (0.000)
Cd_3S_3	2.6618 (0.0274)	1.714	0.9201 (0.000)
Cd_3Se_3	2.5167 (0.0274)	1.449	0.6885 (0.000)
Cd_3Te_3	2.2587 (0.0286)	1.115	0.3940 (0.000)
Hg_3S_3	2.4901 (0.0218)	1.440	0.6322 (0.000)
Hg_3Se_3	2.3381 (0.0213)	1.211	0.4318 (0.000)
Hg_3Te_3	2.0916 (0.0221)	0.914	0.1648 (0.000)

*Only ΔE_{AT} with the greatest oscillator strengths are listed; given in parenthesis after each transition energy is the corresponding oscillator strength.

Correspondingly, there is no resonance observed in experimental absorption spectra. In order to investigate the transition properties of the clusters, the allowed transition energies (ΔE_{AT}), HOMO–LUMO gap energies (ΔE_G) at ground state cluster, and the energy deference between ground state and first excitation state of cluster (ΔE_{FT}) were computed. The corresponding results are listed in Table 2. From these, it can be found that ΔE_{FT} decreases with the increasing of the anionic radius in the order of $\Delta E_{FT}(Zn_3O_3) > \Delta E_{FT}(Zn_3S_3) > \Delta E_{FT}(Zn_3Se_3) > \Delta E_{FT}(Zn_3Te_3)$, $\Delta E_{FT}(Cd_3S_3) > \Delta E_{FT}(Cd_3Se_3) > \Delta E_{FT}(Cd_3Te_3)$ and $\Delta E_{FT}(Hg_3S_3) > \Delta E_{FT}(Hg_3Se_3) > \Delta E_{FT}(Hg_3Te_3)$. And the ΔE_{FT} decrease with the increasing of the metal ionic radius as the same anion in the order of $\Delta E_{FT}(Zn_3S_3) > \Delta E_{FT}(Cd_3S_3) > \Delta E_{FT}(Hg_3S_3)$, $\Delta E_{FT}(Zn_3Se_3) > \Delta E_{FT}(Cd_3Se_3) > \Delta E_{FT}(Hg_3Se_3)$, $\Delta E_{FT}(Zn_3Te_3) > \Delta E_{FT}(Cd_3Te_3) > \Delta E_{FT}(Hg_3Te_3)$. These features can be traced back to the change of ΔE_G, which has the same trend with that for ΔE_{FT}. However, the ΔE_{FT} values are smaller than ΔE_G values, which were identified for the other clusters.[14] We found the evolutions of ΔE_{AT} with a function of the ionic radius have the same orders in those clusters. Thus, the cluster with larger ionic radius would obtain a lower ΔE_{AT}, ΔE_{FT}, and ΔE_G than other clusters in this paper. On the other hand, from Table 2, the evolutions of oscillator strength are not sensitive to change of the ionic radius. It is well known that a well-performing NLO chromophore should possess a low-energy CT excited state with large oscillator strength. According to the results mentioned above, those clusters with large ionic radius would generate a large second-order NLO response.

To investigate the second-order NLO properties, the β values are calculated by SOS formalism. All the contribution of various states are summed up without perturbation. Actually, we only choose finite states to simulate the infinite ones.

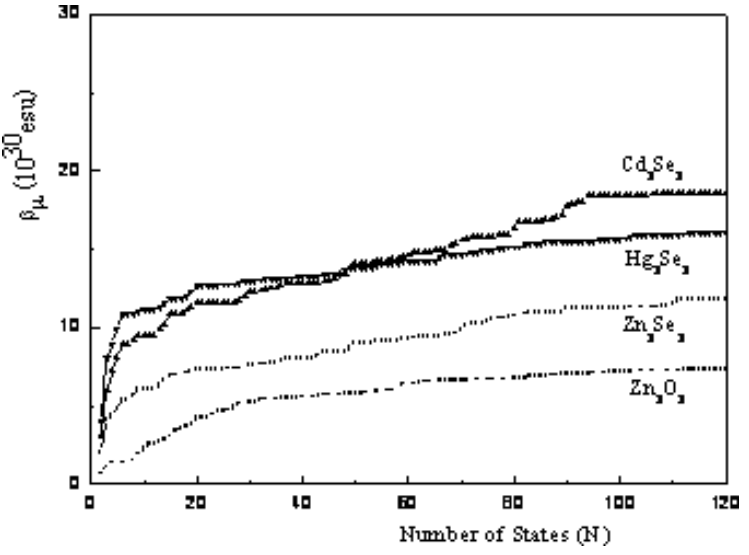

Fig. 3. Convergence behavior of β_μ for Zn_3O_3, Zn_3Se_3, Cd_3Se_3, and Hg_3Se_3 clusters based on TD-B3LYP/CEP-121G level.

Thus, it is necessary to investigate the behavior of the convergence in the summation of excited states. Figure 3 shows a plot of number of excited-states versus the dipole-projected (β_μ) for four representative clusters (Zn_3O_3, Zn_3Se_3, Cd_3Se_3, and Hg_3Se_3) at zero fields. β_μ was obtained by using the following formula:

$$\begin{aligned} \beta_\mu &= (\mu_x\beta_x + \mu_y\beta_y + \mu_z\beta_z)/(\mu_x^2 + \mu_y^2 + \mu_z^2)^{\frac{1}{2}}, \\ \beta_j &= \beta_{jjj} + \frac{1}{3}\sum_{i\neq j}(\beta_{jii} + 2\beta_{ijj}) \quad i,\ j = x, y, z. \end{aligned} \tag{2}$$

It is found from Fig. 3 that the β_μ converged after summation over 60 states for the clusters Zn_3O_3, Zn_3Se_3, and Hg_3Se_3. All the other clusters investigated in this work were found to display a similar convergence behavior, except for Cd_3Se_3 whose convergence is slowly reached after a summation over 90 states. Accordingly, it is reliable to calculate the second-order polarizabilities including 120 excited states, based on the SOS//TD-DFT method. The computed β_μ values for the 10 clusters are listed in Table 3. From these results, one may find that within the same cation,

Table 3. SOS//TD-B3LYP/CEP-121G calculated β_μ($\times 10^{-30}$ esu*) values for II–VI semiconductor clusters.

Clusters	Zn_3O_3	Zn_3S_3	Zn_3Se_3	Zn_3Te_3	Cd_3S_3	Cd_3Se_3	Cd_3Te_3	Hg_3S_3	Hg_3Se_3	Hg_3Te_3
β_μ	7.32	9.70	11.85	17.29	15.59	18.64	24.41	13.16	15.98	26.86

*1 a.u = 8.6392×10^{-33} cm^4 statvolt^{-1} (esu).[19]

β_μ increases with the increase of the anionic radius in the II–VI semiconductor clusters. Then, the variation of β_μ values shows a trend behaving inversely to the one observed with the lowest transition energies and the HOMO–LUMO gap energies discussed above: the smaller is the gap/transition energy, the larger is the second-order NLO response. The first 10 excited-states of the II–VI semiconductor clusters have mainly contribution to β_μ values as shown in Fig. 3.

According to the computational results based on TD-B3LYP method, the excited states arise from electronic transitions involving the frontier molecular orbitals (FMOs). A careful analysis of the FMOs may be then useful for a good interpretation of the optical properties. Figure 4 shows the highest three occupied orbitals and the lowest three unoccupied orbitals of Hg_3S_3 cluster taken as a representative case. In general, the three highest occupied orbitals are found to be mainly made of p_z orbitals from the three S atoms nonlinearly overlapping with the d_{xz} ones from the three Hg atoms. These are considered as weak π bonding molecular orbitals with partial properties of σ orbitals. Similarly, the three lowest unoccupied orbitals were predicted to mainly arise from the S, p_z orbitals of three Hg atoms and the p_z of the S atoms, and are then considered as weak π antibonding molecular orbitals. The FMOs of the other clusters are also similar to those of Hg_3S_3. Consequently, we can infer that the most origin of the second-order NLO

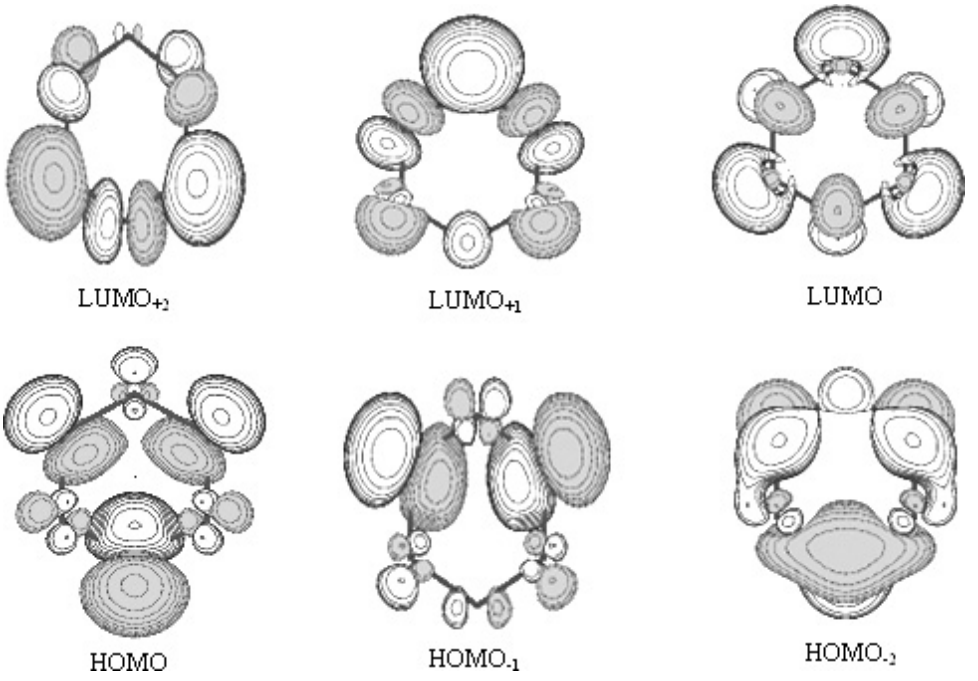

Fig. 4. The highest three occupied orbitals and the lowest three unoccupied orbitals of Hg_3S_3 cluster.

arises from charge transfer from the π bonding to π anti-bonding orbitals between II and VI group atoms in the A_3B_3 semiconductor clusters.

4. Conclusion

We have used the TD-B3LYP method combined with SOS formula to investigate the electronic spectra and second-order NLO properties of 10 A_3B_3 II–VI semiconductor clusters. From our results, the following series of remarkable conclusions can be drawn: (1) For clusters standing from the same cation, the HOMO–LUMO energy gaps and transition energies decrease, and the second-order nonlinear polarizabilities β_μ increase as VI-group anionic radius increase. (2) The charge transfer from the π bonding to the π anti-bonding orbitals contributes a lot to the second-order NLO properties for the A_3B_3 II–VI semiconductor clusters. (3) In general, the calculated results show that the convergence of β_μ for the clusters A_3B_3 is reached after summation over about 60 states, except for Cd_3Se_3 whose convergence is slowly reached after a summation over 90 states.

Acknowledgments

This investigation was supported by the National Natural Science Foundation of China (No. 60376009 and 60576040) and the foundation of Jilin provincial Excellent Youth (Grant No. 20050107).

References

1. Cao H, Xu JY, Zhang DZ, Chang SH, Ho ST, Seelig EW, Liu A, Chang RPH, *Phys Rev Lett* **84**:5584, 2000.
2. Pan ZW, Dai ZR, Wang ZL, *Science* **291**:1947, 2001.
3. Huang MH, Mao S, Feick H, Yan HQ, Wu YY, Kind H, Weber S, Russo R, Yang PD, *Science* **292**:1897, 2001.
4. Service RF, *Science* **276**:895, 1997.
5. Li Y, Meng GW, Zhang LD, Phillipp F, *Appl Phys Lett* **76**:2011, 2000.
6. Li JF, Yao LZ, Ye CH, Mo CM, Cai WL, Zhang Y, Zhan DJ, *Cryst Growth* **223**:535, 2001.
7. Kahamuni S, Borgohain K, Bendre BS, Leppert VJ, Risbud SH, *J Appl Phys* **85**:2861, 1999.
8. Jarrold MF, *Science* **252**:1085, 1991.
9. Mélinon P, Kéghélian P, Prével B, Perez A, Guiraud G, LeBrusq J, Lermé J, Pellarin M, Broyer M, *J Chem Phys* **107**:10278, 1997.
10. Ohara PC, Leff DV, Heath JR, Gelbart WM, *Phys Rev Lett* **75**:3466, 1995.
11. Motte L, Biloudet F, Lacaze E, Pileni MP, *Adv Mater* **8**:1018, 1996.
12. Korambath PP, Karna SP, *J Phys Chem A* **104**:4801, 2000.
13. Vasiliev I, Õgüt S, Chelikowsky JR, *Phys Rev B* **60**:8477, 1999.
14. Lan YZ, Cheng WD, Wu DS, Li XD, Zhang H, Gong YJ, *Chem Phys Lett* **372**:645, 2003.
15. Frisch MJ, Trucks GW, Schlegel HB, Scuseria GE, Robb MA, Cheeseman JR, Montgomery JA, Jr., Vreven T, Kudin KN, Burant JC, Millam JM, Iyengar SS,

Tomasi J, Barone V, Mennucci B, Cossi M, Scalmani G, Rega N, Petersson GA, Nakatsuji H, Hada M, Ehara M, Toyota K, Fukuda R, Hasegawa J, Ishida M, Nakajima T, Honda Y, Kitao O, Nakai H, Klene M, Li X, Knox JE, Hratchian HP, Cross JB, Adamo C, Jaramillo J, Gomperts R, Stratmann RE, Yazyev O, Austin AJ, Cammi R, Pomelli C, Ochterski JW, Ayala PY, Morokuma K, Voth GA, Salvador P, Dannenberg JJ, Zakrzewski VG, Dapprich S, Daniels AD, Strain MC, Farkas O, Malick DK, Rabuck AD, Raghavachari K, Foresman JB, Ortiz JV, Cui Q, Baboul AG, Clifford S, Cioslowski J, Stefanov BB, Liu G, Liashenko A, Piskorz P, Komaromi I, Martin RL, Fox DJ, Keith T, Al-Laham MA, Peng CY, Nanayakkara A, Challacombe M, Gill PMW, Johnson B, Chen W, Wong MW, Gonzalez C, Pople JA, Gaussian 03, Revision C02; Gaussian, Inc., Wallingford, CT, 2004.

16. Stevens WJ, Basch H, Krauss MJ, *Chem Phys* **81**:6026, 1984.
17. Cundari TR, Stevens WJ, *J Chem Phys* **98**:5555, 1993.
18. Orr BJ, Ward JF, *Mol Phys* **20**:513, 1971.
19. Shelton DP, Rice JE, *Chem Rev* **94**:3, 1994.